

Resonance Raman Frequencies and Core Size for Low- and High-Spin Nickel Porphyrins

Dongho Kim,[†] Y. Oliver Su, and Thomas G. Spiro*

Received March 17, 1986

Resonance Raman (RR) spectra are reported with B- and Q-band excitation for nickel(II) complexes of octaethylporphyrin (OEP), protoporphyrin IX dimethyl ester (PP), and *meso*-tetraphenylporphine (TPP) in methylene chloride (4-coordinate, low spin) and piperidine (pip) (6-coordinate, high spin). The large core size expansion accompanying the formation of the 6-coordinate species (1.96–2.04 Å) is reflected in large decreases, up to 40 cm⁻¹ in the positions of high-frequency porphyrin skeletal modes. For NiOEP and NiPP, these are in near-quantitative accord with the core size correlations obtained previously for iron porphyrin complexes, although certain deviations due to differential coupling with the vinyl modes of protoporphyrin are noted. Contributions of a minority 5-coordinate complex to the RR spectrum of NiTPP in piperidine, previously noted on the basis of photolysis effects, are evaluated quantitatively from titration data. Formation of a monopiperidine adduct, detected previously via a RR study of NiTPP(pip)₂ photolysis, is examined for nickel *meso*-tetrakis(*p*-cyanophenyl)porphine. Equilibrium constants for successive addition of piperidine ligands, $K_1 = 0.4$ and $K_2 = 2.5 \text{ M}^{-1}$, are evaluated from optical titration data, and the absorptivities of the 5- and 6-coordinate species are found to be nearly the same, consistent with both having a high-spin configuration. The frequency of the 5-coordinate ν_4 RR band is likewise found to be much closer to the 6-coordinate than to the 4-coordinate frequency.

Introduction

In the course of examining photodeligation reactions of nickel porphyrins using resonance Raman (RR) spectroscopy as a probe,¹ we became interested in the spectral changes associated with the ligation equilibria. Nickel porphyrins are ordinarily 4-coordinate and planar,² although a ruffled form of NiOEP (OEP = octaethylporphyrin) is known.³ When dissolved in strongly ligating solvents, such as pyridine or piperidine, the nickel porphyrins become largely 6-coordinate and high-spin, the electronic rearrangement being forced by the increasing energy of the d_{z^2} orbital induced by the axial ligation.⁴ The change in spin state is accompanied by a substantial increase in the Ni–N(pyrrole) distance, ~0.08 Å, due to the promotion of an electron to the formerly unoccupied in-plane $d_{x^2-y^2}$ orbital.⁵

The core size is known to affect the positions of the high-frequency porphyrin skeletal modes in the RR spectra.⁶ For iron protoporphyrin (PP) complexes negative linear correlations with the porphyrin C_r–N (center-to-nitrogen) distance have been found.⁷ The slopes vary roughly with the contribution of the methine bridge bond stretching coordinates to the normal-mode potential energy distribution,^{8a,b} consistent with the idea that as the porphyrin core expands, the strain is absorbed at the methine bridges,^{8c} resulting in lowering of the methine force constants and of the skeletal mode frequencies. It can be expected that ligation of nickel porphyrins would produce downshifts in these frequencies due to the core size expansion. This is indeed observed in the present study. Dramatic differences are seen for Ni porphyrin complexes dissolved in piperidine or in methylene chloride. When the bands are properly assigned, with different excitation wavelengths and polarization measurements to distinguish overlapping features, the frequency changes for OEP and PP are in near-quantitative accord with those calculated on the basis of the PP core size correlations. Certain deviations are noted, however, that reflect differential coupling of the highest frequency skeletal modes with the vinyl C=C stretching modes of protoporphyrin.

Our photodeligation study¹ gave evidence that 5-coordinate as well as 4-coordinate NiTPP is formed when (pip)₂NiTPP (pip = piperidine) is photolyzed. The 5-coordinate RR band detected in this way is shown in the present study to be overlapped with another band due to the 6-coordinate complex. The equilibrium fraction of 5-coordinate species formed at any piperidine concentration is found to be very small for NiTPP, but for Ni[TPP(CN)₄] (TPP(CN)₄ = *meso*-tetrakis(*p*-cyanophenyl)porphine), this fraction is appreciable at 1 M piperidine, and the 5-coordinate RR band has been characterized via polarization measurements. Optical titration data have been used to calculate equilibrium

constants for successive piperidine addition to Ni[TPP(CN)₄], and the absorptivities for the 5-coordinate species are close to those of the 6-coordinate species, consistent with both of them being high spin. The RR frequencies also support this view.

Since submission of this paper Shelnutt et al.⁹ have reported 4- and 6-coordinate NiPP RR spectra that are in good agreement with ours and also spectra of Ni-substituted myoglobin and hemoglobin, which allow RR characterization of the 5-coordinate NiPP complex formed by coordination of the proximal histidine ligand.

Experimental Section

Nickel complexes of octaethylporphyrin, protoporphyrin IX dimethyl ester, *meso*-tetraphenylporphine, and *meso*-tetrakis(*p*-cyanophenyl)porphine were purchased from Porphyrin Products (Logan, UT) and used without further purification. They were dissolved in spectral grade solvents, and the UV–vis absorption spectra were checked. Raman spectra were obtained via back-scattering from spinning NMR tubes with a Spex 1401 double monochromator, equipped with a cooled photomultiplier and photon-counting electronics, with laser excitation at 406.7, 413.1, 530.9 (Kr⁺), or 441.6 (He–Cd) nm. The data were collected digitally with a MINC (DEC) computer.

Results and Discussion

A. Core Size and Spin State. Figures 1–4 show RR spectra in the 1200–1700-cm⁻¹ region for NiOEP (OEP = octaethylporphyrin) and for NiPP (PP = protoporphyrin IX dimethyl ester) in methylene chloride and in piperidine with laser excitation at 413.1 nm, in the region of the B absorption bands, or at 530.9 nm, in the region of the Q bands. In methylene chloride, NiOEP

- (1) Kim, D.; Spiro, T. G. *J. Am. Chem. Soc.* **1986**, *108*, 2099.
- (2) Cullen, D. L.; Meyer, E. F., Jr. *J. Am. Chem. Soc.* **1974**, *96*, 2095. Hamor, T. A.; Caughey, W. S.; Hoard, J. L. *J. Am. Chem. Soc.* **1965**, *87*, 2305. Fleischer, E. B. *J. Am. Chem. Soc.* **1963**, *85*, 146.
- (3) Meyer, E. F., Jr. *Acta Crystallogr., Sect. B: Struct. Crystallogr. Cryst. Chem.* **1972**, *B28*, 2162.
- (4) (a) McLees, D. D.; Caughey, W. S. *Biochemistry* **1968**, *7*, 642. (b) La Mar, G. N.; Walker, F. A. In *The Porphyrins*; Dolphin, D., Ed.; Academic: New York, 1978; Vol. 4, p 61. (c) Abraham, R. J.; Swinton, P. F. *J. Chem. Soc. B* **1969**, *8*, 903.
- (5) Kirner, J. F.; Garofollow, J., Jr.; Scheidt, W. R. *Inorg. Nucl. Chem. Lett.* **1975**, *11*, 107.
- (6) (a) Spaulding, L. D.; Chang, C. C.; Yu, N. T.; Felton, R. H. *J. Am. Chem. Soc.* **1975**, *97*, 2519. (b) Huong, P. V.; Pommier, J.-C. *C. R. Seances Acad. Sci., Ser. C* **1977**, *285*, 519. (c) Spiro, T. G.; Stong, J. D.; Stein, P. *J. Am. Chem. Soc.* **1979**, *101*, 2648.
- (7) Choi, S.; Spiro, T. G.; Langry, K. C.; Smith, K. M.; Budd, D. L.; La Mar, G. N. *J. Chem. Soc.* **1982**, *104*, 4345.
- (8) (a) Kitagawa, T.; Abe, M.; Ogoshi, H. *J. Chem. Phys.* **1978**, *69*, 4516. (b) Abe, M.; Kitagawa, T.; Kyogoku, Y. *Ibid.* **1978**, *69*, 4526. (c) Warshel, A. *Rev. Biophys. Bioeng.* **1977**, *6*, 273.
- (9) Shelnutt, J. A.; Alston, K.; Ho, J.-Y.; Yu, N.-T.; Yamamoto, T.; Rifkind, J. M. *Biochemistry* **1986**, *25*, 620.

* To whom correspondence should be addressed.

[†] Present address: Korea Institute of Standards, Daedok Science Town 300-31, Taejeou, Korea.

Table I. RR Frequencies (cm^{-1}) for Nickel Octaethylporphyrin and Protoporphyrin

mode ^a	NiOEP	ν_{calcd}^b (1.958 Å)	NiPP	(pip) ₂ NiOEP	ν_{calcd}^b (2.038 Å)	(pip) ₂ NiPP
ν_{10} (B_{1g})	1655	1656	1655	1612	1614	1604
$\nu_{C=C}$			1634			1630 1620
ν_{37} (E_u)		1611	1609		1583	1583
ν_{19} (A_{2g})	1602	1603	1602	1559	1563	<i>d</i>
ν_2 (A_{1g})	1600	1591	1593	1586	1560	1566 ^c
ν_{11} (B_{1g})	1575	1576	1578	<i>d</i>	1549	1554
ν_{38} (E_u)		1568	1566		1524	1531
ν_3 (A_{1g})	1519	1521	1519	1480	1485	1480
ν_{28} (B_{2g})	1483	1481	1483	<i>d</i>	1449	<i>d</i>
ν_{29} (B_{2g})	1407		1407	1396		1402
ν_4 (A_{1g})	1382	1381	1381	1370	1371	1368
ν_{20} (A_{2g})	1397	1399	1384			1393
$\delta_s = \text{CH}_2$ (2)			1343			1337
ν_{21} (A_{2g})	1308	1305	1318			1308
$\nu_5 + \nu_9$ (A_{1g})	1260	1254	1258			1248
ν_{13} (B_{1g})	1219	1234	1211			1218

^a Assignments from ref 8 and 10. ^b Calculated frequencies for the indicated core size (C_i-N) from $\nu_{\text{calcd}} = K(A-d)$, where $d = C_i-N$ (Å) and K (A) = 517.2 (5.16), 356.3 (6.48), 494.3 (5.20), 390.8 (6.03), 344.8 (6.53), 551.7 (4.80), 448.3 (5.35), 402.3 (5.64), and 133.3 (12.32) for ν_{10} , ν_{37} , ν_{19} , ν_2 , ν_{11} , ν_{38} , ν_3 , ν_{28} , and ν_4 , respectively (parameters obtained for Fe protoporphyrin complexes.^{7,19} ^c Frequency uncertain due to expected overlap with ν_{37} (calcd 1563 cm^{-1}). ^d Obscured by nearby bands.

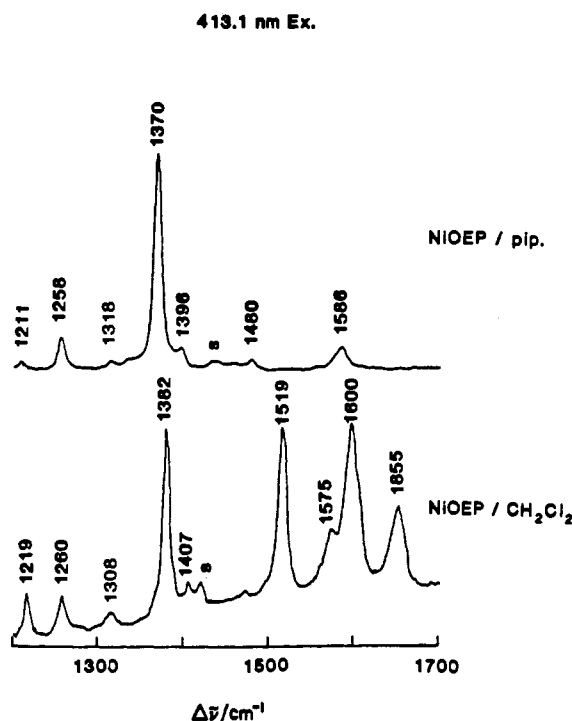


Figure 1. RR spectra with B-band excitation (413.1 nm) for NiOEP (0.1 mM) in methylene chloride and in piperidine. Conditions: laser power, 100 mW; slit width, 6 cm^{-1} ; scan rate, 0.5 cm^{-1}/s .

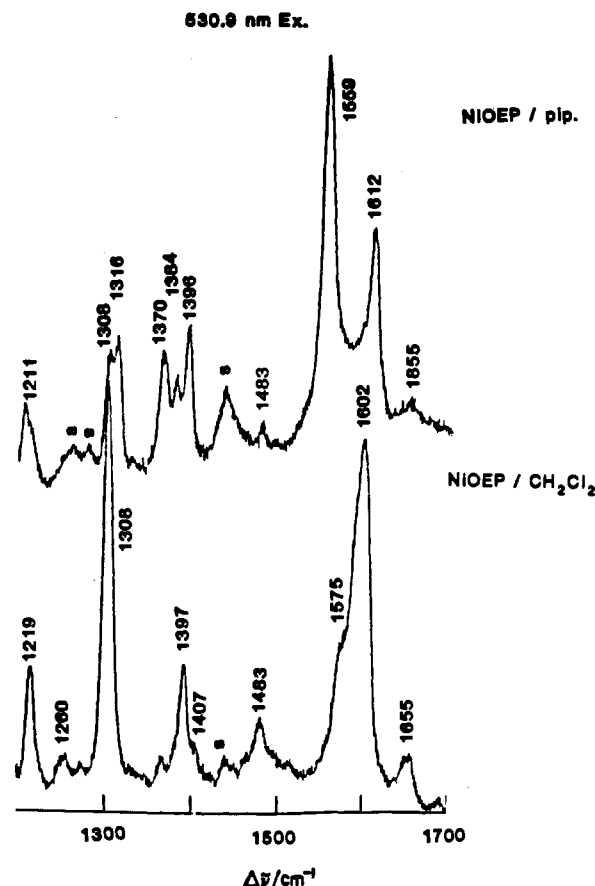


Figure 2. RR spectra with Q-band excitation (530.9 nm) for NiOEP (0.1 mM) in methylene chloride and in piperidine. Conditions are as in Figure 1.

and NiPP are 4-coordinate and low spin. The porphyrin vibrational modes giving rise to the RR bands have been analyzed via isotopic studies in ref 7 and 8a. The present spectra are in agreement with these assignments, which are given in Table I.

NiOEP crystallizes in two forms, containing planar (D_{4h}) or ruffled (D_{2d}) porphyrin structures. The solution spectra are close to those given by the crystals containing planar NiOEP. In the D_{4h} molecular symmetry, the in-plane porphyrin skeletal vibrations classify as A_{1g} , A_{2g} , B_{1g} , and B_{2g} . Excitation in the neighborhood of the strongly allowed B absorption bands produces strong enhancement of Franck-Condon-active A_{1g} modes, while excitation in the neighborhood of the quasi-forbidden Q bands produces selective enhancement of vibronically active A_{2g} , B_{1g} , and B_{2g} modes.¹⁰ This is the pattern displayed by our NiOEP spectra

(Figures 1 and 2). The 413.1-nm laser line is 20 nm to the red of the B-band maximum, 393 nm. In addition to the strongly enhanced A_{1g} modes (ν_2 , ν_3 , and ν_4 at 1600, 1519, and 1382 cm^{-1}), appreciable intensity is seen for B_{1g} (ν_{10} , ν_{11} , and ν_{13} at 1655, 1575, and 1219 cm^{-1}), B_{2g} (ν_{29} at 1407 cm^{-1}), and A_{2g} (ν_{21} at 1308 cm^{-1}) modes, attributable to residual enhancement via the lower energy Q bands. The 530.9-nm laser line lies between the Q_0 (562 nm) and Q_1 (515 nm) bands. A_{1g} modes are now nearly undetectable (Figure 2), while the nontotally symmetric modes are enhanced, particularly the A_{2g} modes (ν_{19} , ν_{20} , and ν_{21} at 1602, 1397, and 1308 cm^{-1}). (The $A_{2g}/B_{1g,2g}$ intensity ratio is expected to maximize

(10) Spiro, T. G. In *Iron Porphyrins*; Lever, A. B. P., Gray, H. B., Eds.; Addison-Wesley: Reading, MA, 1983; Part II, p 89.

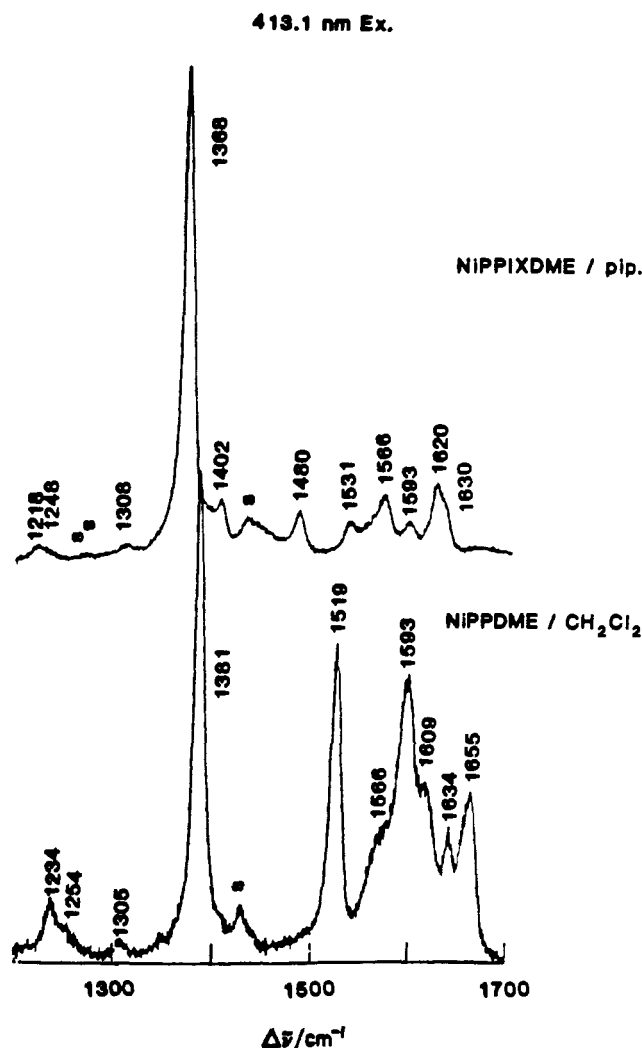


Figure 3. RR spectra with B-band excitation (413.1 nm) for NiPP (0.1 mM) in methylene chloride and in piperidine. Conditions are as in Figure 1.

between Q_0 and Q_1 due to differential interference effects between these two electronic levels.¹¹)

The enhancement pattern is similar for NiPP, but the vinyl substituents introduce additional features.¹² These include enhancement of vibrational modes of the vinyl groups themselves: $\nu_{C=C}$ at 1634 cm^{-1} , seen in B-band excitation, and a vinyl scissors mode at 1343 cm^{-1} , seen with Q-band excitation. (Another vinyl scissors mode is expected at 1425 cm^{-1} with B-band excitation,¹² but it is obscured in our spectrum by a solvent band.) In addition the asymmetric disposition of the vinyl groups induces RR activity for E_u modes, particularly ν_{37} and ν_{38} at 1609 and 1566 cm^{-1} . Finally, the frequencies of skeletal modes ν_2 and ν_{29} are shifted significantly, relative to NiOEP, via interaction with the vinyl modes.¹²

When nickel porphyrins are dissolved in piperidine, coordination of the solvent produces a 6-coordinate high-spin adduct.^{4,13} The position of this equilibrium varies somewhat with the porphyrin,¹³ and there is always some 4-coordinate low-spin complex in solution. Its influence on the RR spectra depends on the resonance matching of the laser wavelength to the absorption spectra of the high- and low-spin species. For example, with 530.9-nm excitation (Figure

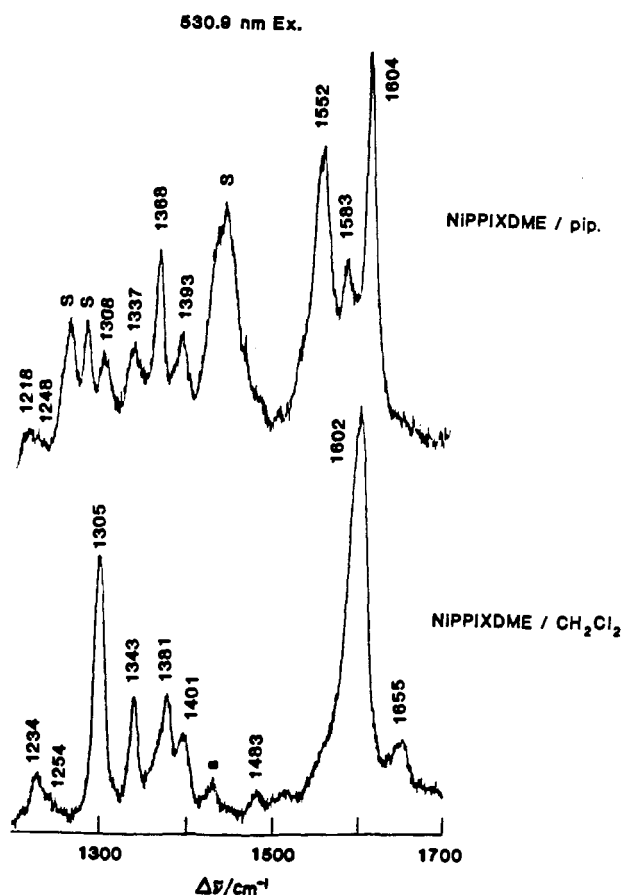


Figure 4. RR spectra with Q-band excitation (530.9 nm) for NiPP (0.1 mM) in methylene chloride and in piperidine. Conditions are as in Figure 1.

2) residual 4-coordinate NiOEP peaks can be seen in the piperidine spectrum at 1655 , 1483 , and 1308 cm^{-1} . On the other hand, with 413.1-nm excitation (Figure 1) no 4-coordinate contribution can be observed, since the frequency is much closer to resonance with the high-spin (419 nm) than the low-spin (393 nm) B-band maximum.

The RR features of the high-spin species are readily observed in these spectra and can easily be correlated with the low-spin bands via the wavelength-intensity relationships. An observation of some interest is that NiPP in pyridine shows a band at 1620 cm^{-1} , with a shoulder at 1630 cm^{-1} , with 413.1-nm excitation. Neither component of this band is due to skeletal mode ν_{10} , which shows up clearly at 1604 cm^{-1} in the 530.9-nm-excited spectrum; all other skeletal modes are at lower frequency. We assign the $1620/1630\text{ cm}^{-1}$ modes to vinyl C=C stretching. Two such modes are expected, and a $\sim 15\text{ cm}^{-1}$ splitting between them was noted for 4-coordinate NiPP by comparing Raman and infrared spectra.¹² The low-frequency component, at 1620 cm^{-1} , is not seen in the NiPP RR spectrum but evidently becomes enhanced for $(\text{pip})_2\text{NiPP}$.

Assignments for the bis(piperidine) adducts are given in Table I. The recent data of Shelnutz et al.⁹ are in accord with the NiPP frequencies. There is a systematic lowering of the high-frequency skeletal modes relative to NiOEP and NiPP. This trend is as expected on the basis of core size considerations. In the high-spin bis(piperidine) adducts an electron is forced into the antibonding $d_{x^2-y^2}$ in-plane orbital, whereas in the low-spin 4-coordinate complexes this orbital is empty. The partial occupancy of the $d_{x^2-y^2}$ orbital results in a substantial lengthening of the Ni-N(pyrrole) bonds and an expansion of the porphyrin. The bond distance is 2.038 \AA for the bis(imidazole) adduct of tetrakis(*N*-methylpyridiniumyl)porphine⁵ but averages 1.958 \AA for three planar nickel porphyrins (1.958 \AA for NiOEP,^{2a} 1.960 \AA for nickel deuteroporphyrin,^{2b} and 1.957 \AA for nickel etioporphyrin^{2c}). For a series of iron protoporphyrin complexes, the frequencies of all

(11) (a) Shelnutz, J. A.; Cheung, L. D.; Chang, R. C. C.; Yu, N.-T.; Felton, R. H. *J. Chem. Phys.* **1977**, *66*, 3387-3398. (b) Spiro, T. G.; Stein, P. *Annu. Rev. Phys. Chem.* **1977**, *28*, 501-21.

(12) Choi, S.; Spiro, T. G.; Langry, K. C.; Smith, K. M. *J. Am. Chem. Soc.* **1982**, *104*, 4337.

(13) Walker, F. A.; Hui, E.; Walker, J. M. *J. Am. Chem. Soc.* **1975**, *97*, 2390.

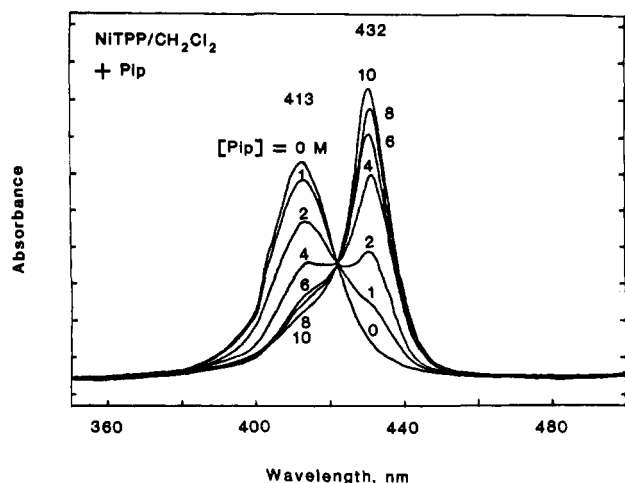


Figure 5. B-Band absorption spectra for NiTPP (4.83×10^{-6} M) in methylene chloride with successively larger concentrations of added piperidine up to pure piperidine (10 M).

of the skeletal modes above 1450 cm^{-1} and also of ν_4 at $\sim 1360 \text{ cm}^{-1}$ have been found to correlate inversely with the porphyrin core size.⁷

In Table I we list the expected values of these frequencies based on the core size parameters obtained from the iron protoporphyrin correlations⁷ using 1.958 \AA for the 4-coordinate porphyrins and 2.038 \AA for the 6-coordinate porphyrins. The close agreement of calculated and observed values for NiPP is expected, since this molecule, which has a particularly small core, was used to anchor the iron protoporphyrin core size correlations.⁷ For $(\text{pip})_2\text{NiTPP}$ the agreement is still quite good, especially in view of the likelihood that the core size is not quite the same for the bis(piperidine) adduct of NiPP as it is for the bis(imidazole) adduct of Ni-tetrakis(*N*-methylpyridinium)porphine. The largest deviation (10 cm^{-1}) is seen for ν_{10} . Interestingly, the calculated value of this frequency agrees better with that observed for $(\text{pip})_2\text{NiOEP}$ than for $(\text{pip})_2\text{NiPP}$. The ν_{10} frequencies are the same, 1655 cm^{-1} , for NiOEP and NiPP, but they differ by 8 cm^{-1} for the bis(piperidine) adducts. It is possible that this difference is induced by an interaction with the vinyl $\text{C}=\text{C}$ modes, the lower of which (1620 cm^{-1}) is closer to ν_{10} in the 6-coordinate adduct than in the 4-coordinate adduct. The remaining deviations between observed and calculated frequencies for $(\text{pip})_2\text{NiPP}$ are all less than 7 cm^{-1} and are small relative to the large differences between NiPP and $(\text{pip})_2\text{NiPP}$. It is evident that these differences are mainly a result of the expanded porphyrin core in the high-spin 6-coordinate adducts.

B. 5-Coordination in NiTPP-Piperidine. We recently reported RR evidence for laser-induced deligation of NiTPP (TPP = tetraphenylporphine) in pyridine or piperidine.¹ With increasing laser (406.7 nm) power incident on a stationary sample, the 1369-cm^{-1} RR band due to ν_4 of 4-coordinate NiTPP increased at the expense of the 1346-cm^{-1} ν_4 band of the 6-coordinate species. In piperidine solution, an additional band at an intermediate frequency, 1356 cm^{-1} , grew in and was suggested to reflect formation of a 5-coordinate complex. 5-coordinate nickel porphyrins have been elusive, since the coordination equilibria appear to be biased toward 4- or 6-coordinate forms. They are of theoretical interest, however, since it is not obvious whether addition of one ligand to nickel porphyrins is sufficient to force the change from low- to high-spin configuration. Calculations by Ake and Gouterman¹⁴ suggest a high-spin configuration for 5-coordinate species, and the intermediate frequency observed for ν_4 in the photopumping experiment was suggested to be consistent with high-spin character.¹

In order to study the 5-coordinate species more closely, we examined solutions of NiTPP in methylene chloride with increasing

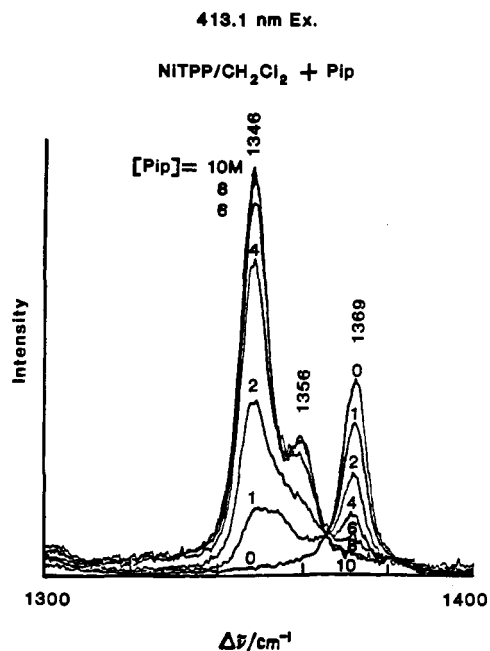


Figure 6. ν_4 region of the NiTPP RR spectrum (413.1-nm excitation) for the same solutions as in Figure 5. Successive spectra are scaled via the 1369-cm^{-1} band in proportion to the 413-nm absorbance.

piperidine concentrations. Absorption spectra in the Soret band region are shown in Figure 5. A sharp isosbestic point is seen at 423 nm , implying that only two components, the 4- and 6-coordinate species, are present in significant amounts over the entire concentration range. Similar data have been reported by Walker et al.,¹³ who determined the equilibrium constant for the addition of two piperidine ligands to NiTPP, β_2 , to be 0.43 M^{-2} in toluene solution. We calculate a value of 0.16 in methylene chloride. By measuring small spectral changes at low equilibrium concentrations, Walker et al. estimated an equilibrium constant of 200 M^{-1} for the addition of one piperidine ligand to NiTPP.¹³ Given the separately measured β_2 , however, this value is inconsistent with formation of any significant amount of the bis(piperidine) adduct, even in pure piperidine (10 M), and must be too high by at least 3 orders of magnitude. Figure 6 shows RR spectra in the region of the ν_4 bands for the same solutions as in Figure 5; the 1369-cm^{-1} 4-coordinate NiTPP intensity being scaled via the absorption spectra. An isosbestic point is again seen. It is clear from this figure that the 1356-cm^{-1} band as well as the 1346-cm^{-1} ν_4 band must be associated with the 6-coordinate species.

We assign the 1356-cm^{-1} band to the ν_{28} (B_{2g}) mode of TPP, which occurs a few wavenumbers higher than ν_4 .¹³ (The intensity of this band with B-band excitation is variable and probably depends on the degree of Jahn-Teller distortion in the excited state;¹⁶ this can vary for different ligands due to shifts in the porphyrin orbital energies and consequent changes in the extent of configuration interaction, which controls the Jahn-Teller splitting.) This assignment is confirmed by the polarization spectra shown in the left-hand panel of Figure 7. Clearly, the 1346-cm^{-1} band is more polarized than the 1356-cm^{-1} band. The depolarization ratios are 0.22 and 0.53 , respectively. A ratio of 0.75 is expected for a B_{2g} mode, and the smaller observed ratio suggests that there is a contribution from a polarized (A_{1g}) mode. We propose that this contribution is from the ν_4 band of the 5-coordinate species, present in small concentration. This coincidence of the 4-coordinate ν_{28} band and the 5-coordinate ν_4 band explains the increase in 1356-cm^{-1} intensity upon photolysis of $(\text{pip})_2\text{NiTPP}$,¹ giving a steady-state concentration of a 5-coordinate

(15) Stein, P.; Ulman, A.; Spiro, T. G. *J. Phys. Chem.* **1984**, *88*, 369.

(16) Cheung, L. D.; Yu, N.-T.; Felton, R. H. *Chem. Phys. Lett.* **1978**, *55*, 527.

(14) Ake, R. L.; Gouterman, M. *Theor. Chim. Acta* **1970**, *17*, 408.

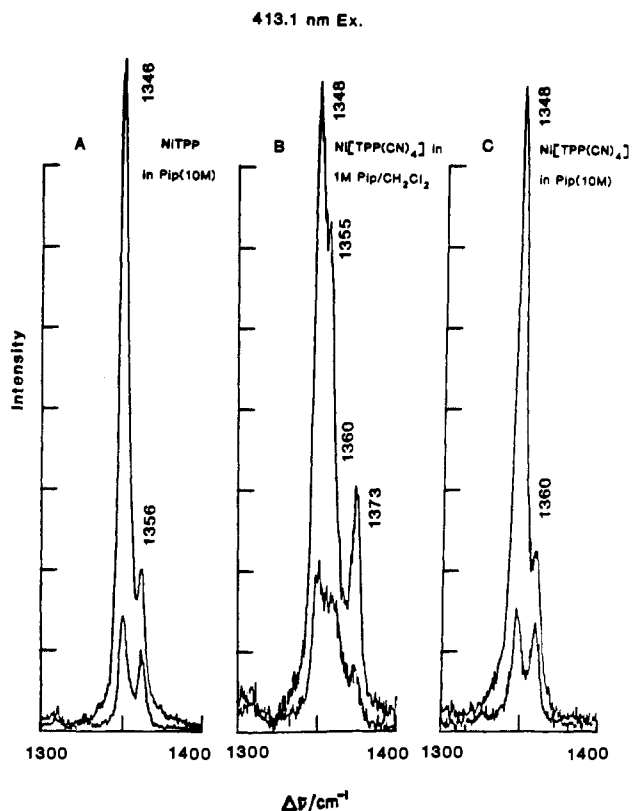


Figure 7. 413.1-nm-excited RR spectra in parallel (top) and perpendicular (bottom) polarization for NiTPP in piperidine (left panel) and for Ni[TPP(CN)₄] in piperidine (right panel) and in CH₂Cl₂ containing 1 M piperidine (center panel). The latter spectrum shows ν_4 bands ($\rho = 0.26$) for 6- (1348 cm⁻¹), 5- (1355 cm⁻¹), and 4-coordinate (1373 cm⁻¹) species. The left and right panels show ν_4 (1346/1348 cm⁻¹) and ν_{28} (1356/1360 cm⁻¹) of the 6-coordinate species.

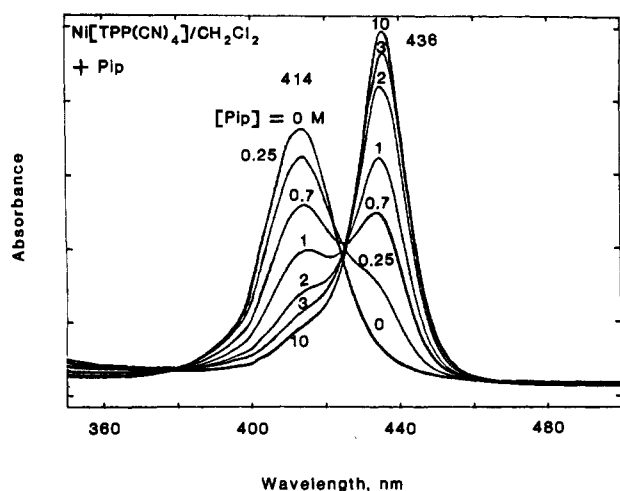


Figure 8. As Figure 5, but for Ni[TPP(CN)₄].

species that is higher than the equilibrium concentration.

In order to examine a 5-coordinate Ni porphyrin more closely, we studied absorption and RR spectra for piperidine adducts with Ni tetrakis(*p*-cyanophenyl)porphine, Ni[TPP(CN)₄], on the theory that the electronic withdrawing cyano groups, which are known to stabilize the bis(piperidine) adduct,¹³ might also stabilize the monopiperidine adduct. This is indeed the case, as demonstrated by the absorption spectra in Figure 8 for Ni[TPP(CN)₄] in methylene chloride at varying piperidine concentrations. There is no longer a clean isosbestic point, indicating that Ni[TPP(CN)₄](pip) is formed in detectable amounts. Moreover, the RR spectra (Figure 9) show pronounced intensity at 1355 cm⁻¹ at relatively low (1 M) piperidine concentration, followed by a di-

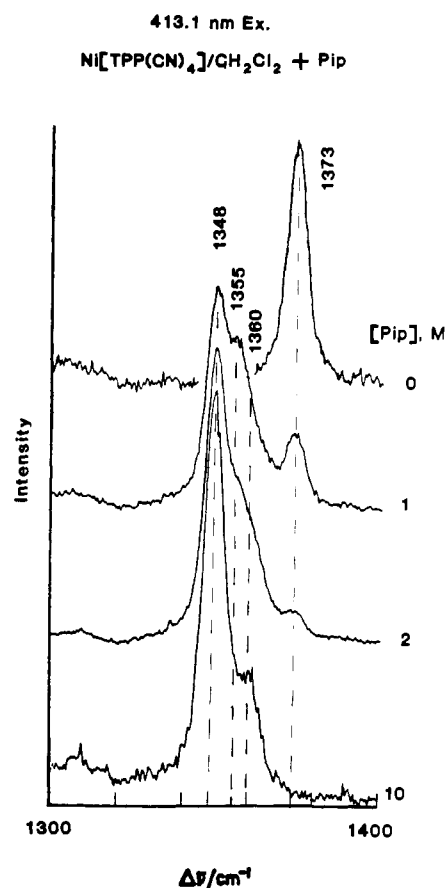


Figure 9. As Figure 6, but for Ni[TPP(CN)₄]. Spectra are displaced for clarity.

minution of this intensity and a shift of the band to 1360 cm⁻¹ at high piperidine concentration. Polarization spectra in 1 M and 10 M piperidine are shown in the middle and right-hand panels of Figure 7. Clearly, the 1355-cm⁻¹ band present in 1 M piperidine is polarized to the same extent ($\rho = 0.26$) as the 1348- and 1373-cm⁻¹ ν_4 bands. On the other hand, the depolarization ratio for the 1360-cm⁻¹ band in 10 M piperidine is significantly higher, 0.52. These results clearly establish that the 5-coordinate complex, Ni[TPP(CN)₄](pip), is present in 1 M piperidine and gives rise to a ν_4 band at 1355 cm⁻¹. It is converted to the 6-coordinate species at higher piperidine concentration, leaving the 1360-cm⁻¹ ν_{28} band of (pip)₂Ni[TPP(CN)₄] exposed.

The absorbance data in Figure 8 were analyzed by successive approximations to give equilibrium constants for the addition of two successive piperidine ligands to Ni[TPP(CN)₄], $K_1 = 0.4$ and $K_2 = 2.5$ M⁻¹ ($\beta_2 = 1.0$ M⁻²). These values give a maximal fraction, ~15%, of the 5-coordinate complex at 1 M piperidine, consistent with the concentration dependence of the RR spectra in Figure 9. The calculated absorptivities for the 5-coordinate complex are nearly the same as those of the 6-coordinate complex, as expected if the 5-coordinate complex is in fact high spin. This conclusion is at variance with the suggestion of Walker et al.¹³ that the 5-coordinate absorption spectrum is essentially the same as that of the 4-coordinate species; this suggestion was, however, based on the analysis of the small absorption changes that produced an unrealistically high value for the 5-coordinate complex formation constant.

The present equilibrium constants provide indirect support for the inference that the 5-coordinate complex is high spin, since K_1 is less than K_2 . The K_1/K_2 ratio must be still smaller for NiTPP since the equilibrium concentration of (pip)NiTPP is undetectable. Thus, the addition of the first piperidine ligand is energetically less favorable than the second, consistent with the expenditure of the extra energy required to promote an electron to the $d_{x^2-y^2}$ orbital in the first ligation step. As noted previously,¹ the ν_4 RR frequency for the 5-coordinate adduct is also consistent with a

high-spin structure. This frequency is much closer to the 6-coordinate than to the 4-coordinate ν_4 position, suggesting a substantial expansion of the porphyrin core on adding the first ligand, due to the $d_{x^2-y^2}$ orbital occupancy. The 7-cm^{-1} upshift relative to ν_4 of the high-spin 6-coordinate adduct can be attributed to partial relaxation of the core size due to the out-of-plane displacement of the Ni atom expected for a high-spin 5-coordinate adduct. A similar relaxation is seen for the 5-coordinate high-spin Fe^{II} complex (2-MeImH)FeTPP (2.45 Å, $\text{C}_1\text{-N}$; Fe 0.5 Å out of plane)¹⁷ relative to the high-spin 6-coordinate adduct (THF)₂-FeTPP (2.57 Å, $\text{C}_1\text{-N}$; Fe in plane).¹⁸ Shelnut et al.⁹ have been

able to determine RR bands for 5-coordinate NiPP from Ni-substituted myoglobin and hemoglobin, in which the proximal histidine side chain provides the single axial ligand. Again the frequencies are intermediate between those of 4- and 6-coordinate complexes.

Acknowledgment. This work was supported by Grant AC02-81ER10861 from the U.S. Department of Energy.

Registry No. Ni(OEP), 24803-99-4; Ni(PP), 15304-70-8; Ni(TPP), 14172-92-0; Ni[TPP(CN)₄], 104129-95-5; Ni[TPP(CN)₄](pip), 104129-96-6; Ni[TPP(CN)₄](pip)₂, 55835-72-8.

(17) Hoard, J. L.; Scheidt, W. R. *Proc. Natl. Acad. Sci. U.S.A.* **1973**, *70*, 3913; **1974**, *71*, 1578.

(18) Reed, C. A.; Mashiko, T.; Scheidt, W. R.; Spartalian, K.; Lang, G. J. *Am. Chem. Soc.* **1980**, *102*, 2302.

(19) Feitelson, J.; Spiro, T. G. *Inorg. Chem.* **1986**, *25*, 861.

Contribution from the Department of Chemistry,
Princeton University, Princeton, New Jersey 08544

Back-Bonding in Ruthenium Porphyrins As Monitored by Resonance Raman Spectroscopy

Dongho Kim,[†] Y. Oliver Su, and Thomas G. Spiro*

Received March 17, 1986

Resonance Raman spectra are reported for Ru^{II} complexes of octaethylporphyrin (OEP) and tetraphenylporphine (TPP) with pyridine, methanol, and CO axial ligands, using both B- and Q-band excitation. For $\text{Ru}^{\text{II}}\text{OEP}(\text{CO})(\text{MeOH})$ the porphyrin skeletal mode frequencies above 1370 cm^{-1} agree remarkably well with the values calculated on the basis of the porphyrin core size by using parameters derived earlier for iron protoporphyrin complexes. These frequencies shift both positively and negatively when the CO is replaced by pyridine due to π -back-donation from Ru to the porphyrin π^* orbitals. The shift pattern is the same as that observed for the bis(imidazole) adduct of iron(II) protoporphyrin, relative to the core size predictions, and the extent of the shifts is very similar in the two cases. Thus, π -back-bonding to the porphyrin appears to be quantitatively similar for Ru^{II} and Fe^{II} . π -Back-bonding shifts are also reported for $\text{Ru}^{\text{II}}\text{TPP}(\text{py})_2$. For $\text{Ru}^{\text{II}}\text{OEP}(\text{CO})(\text{py})$ the Ru-CO stretching, Ru-C-O bending, and C-O stretching modes are observed at 513, 578, and 1930 cm^{-1} . For Fe^{II} porphyrins, the M-CO and C-O frequencies are somewhat lower and higher, respectively, implying greater back-donation to the bound CO for Ru^{II} than for Fe^{II} .

Introduction

Ruthenium porphyrins have recently attracted interest because of their unusual electronic and chemical properties.¹⁻⁶ For Ru^{II} , back-bonding to π -acceptor ligands, including porphyrin itself, is a dominant feature of the chemistry. The situation is similar to that of Fe^{II} porphyrins, which are widespread in nature, and comparisons between the two are instructive. Back-bonding also plays a role in controlling the photoexcitation pathways for Ru^{II} porphyrins.⁶ Thus, when both axial ligands are pyridine, the lowest excited state is short-lived ($\sim 12\text{ ns}$) and is believed to be a $d\text{-}\pi^*$ metal \rightarrow porphyrin charge-transfer state, but when one of the ligands is CO, a longer lived ($\sim 70\text{ }\mu\text{s}$) $^3(\pi\text{-}\pi^*)$ state is formed because back-bonding to the CO raises the energy of the $d\text{-}\pi^*$ state.⁶

In this study we report resonance Raman spectra for CO and pyridine adducts of ruthenium(II) octaethylporphyrin (OEP) and tetraphenylporphine (TPP), with laser excitation in resonance with the B and Q absorption bands. The porphyrin skeletal modes are assigned with reference to the schemes that have been worked out for OEP⁷ and TPP⁸ complexes. Appreciable frequency shifts are associated with the presence or absence of bound CO, consistent with competition for π -back-bonding between the porphyrin and the CO π^* orbitals. The pattern is the same as has been observed for analogous Fe^{II} porphyrins,⁹ and the extent of the shifts is quantitatively similar, suggesting comparable back-bonding to porphyrin from either Ru^{II} or Fe^{II} . The M-CO and C-O stretching frequencies, however, are higher and lower, respectively,

for Ru^{II} than Fe^{II} , implying stronger back-bonding to CO from Ru^{II} .

RR spectra for $\text{RuOEP}(\text{py})_2$ have been reported by Schick and Bocian,⁵ who analyzed excitation profiles for both porphyrin and pyridine modes and compared them with the Fe and Os analogues. They assigned M \rightarrow py charge-transfer transitions in the visible region and calculated excited-state distortions of the py ring, as Wright et al.¹⁰ had done for the bis(pyridine) adduct of iron(II) *meso*-porphyrin. In the present work we have not been concerned with the pyridine enhancements.

Experimental Section

$\text{RuOEP}(\text{CO})(\text{MeOH})$ and $\text{RuTPP}(\text{CO})(\text{MeOH})$ were purchased from Porphyrin Products (Logan, UT) and used without further purification. The bis(pyridine) adducts were prepared by photolyzing the CO adducts in pyridine by using a tungsten lamp with a ultraviolet cutoff

* To whom correspondence should be addressed.

[†] Present address: Korea Institute of Standards, Daedok Science Town 300-31, Taejeou, Korea.

- (1) Collman, J. P.; Barnes, C. E.; Collins, T. J.; Brother, P. J. *J. Am. Chem. Soc.* **1981**, *103*, 7030-7032.
- (2) Antipas, A.; Buchler, J. W.; Gouterman, M.; Smith, P. D. *J. Am. Chem. Soc.* **1980**, *102*, 198-207.
- (3) Antipas, A.; Buchler, J. W.; Gouterman, M.; Smith, P. D. *J. Am. Chem. Soc.* **1978**, *100*, 3015-3024.
- (4) Buchler, J. W.; Kokisch, W.; Smith, P. D. *Struct. Bonding (Berlin)* **1978**, *34*, 79-134.
- (5) Schick, G. A.; Bocian, D. F. *J. Am. Chem. Soc.* **1984**, *106*, 168.
- (6) Tait, C. D.; Holten, D.; Barley, M. H.; Dolphin, D.; James, B. R. *J. Am. Chem. Soc.* **1985**, *107*, 1930.
- (7) (a) Kitagawa, T.; Abe, M.; Ogoshi, H. *J. Chem. Phys.* **1978**, *69*, 4516. (b) Abe, M.; Kitagawa, T.; Ogoshi, H. *J. Chem. Phys.* **1978**, *69*, 4526.
- (8) Stein, P.; Ulman, A.; Spiro, T. G. *J. Phys. Chem.* **1984**, *88*, 369.
- (9) Choi, S.; Spiro, T. G.; Langry, K. C.; Smith, K. M.; Budd, D. L.; LaMar, G. N. *J. Am. Chem. Soc.* **1982**, *104*, 4345.
- (10) Wright, P. G.; Stein, P.; Burke, J. M.; Spiro, T. G. *J. Am. Chem. Soc.* **1979**, *101*, 3531.